

conservative test for the effect of temperature on rates of phenotypic evolution.

We applied our climatic models to rates of body size evolution in birds and mammals (*Materials and Methods*). We used the two most up to date species-level phylogenies for mammals (20, 21), but these phylogenies are less reliable than the bird phylogeny, in particular with respect to their branch lengths. We thus focus on the bird results, with the mammal results presented in *SI Appendix*. We found similar trends for the two groups. Our climatic model with exponential dependency of evolutionary rates to temperature (Clim-exp) was better supported than all other models for most groups (Fig. 1 and *SI Appendix*, Figs. S16–S18). Anecdotally, groups restricted to regions that have been relatively climatically stable in the last several million years, such as the tropics (the neotropical bird families Thamnophilidae and Ramphastidae and the Primates) and Oceania (Meliphagidae, Diprotodontia, and Dasyuromorphia), supported other models than the climatic ones.

Estimated β values were negative, indicating a consistent trend for a slowdown in rates of body size evolution during periods of climate warming (Fig. 2 and *SI Appendix*, Figs. S16–S18). The only few groups that showed a tendency toward positive β values (Procellariiformes, Thamnophilidae, Meliphagidae, Ramphastidae, and the Primates) were groups for which climatic models

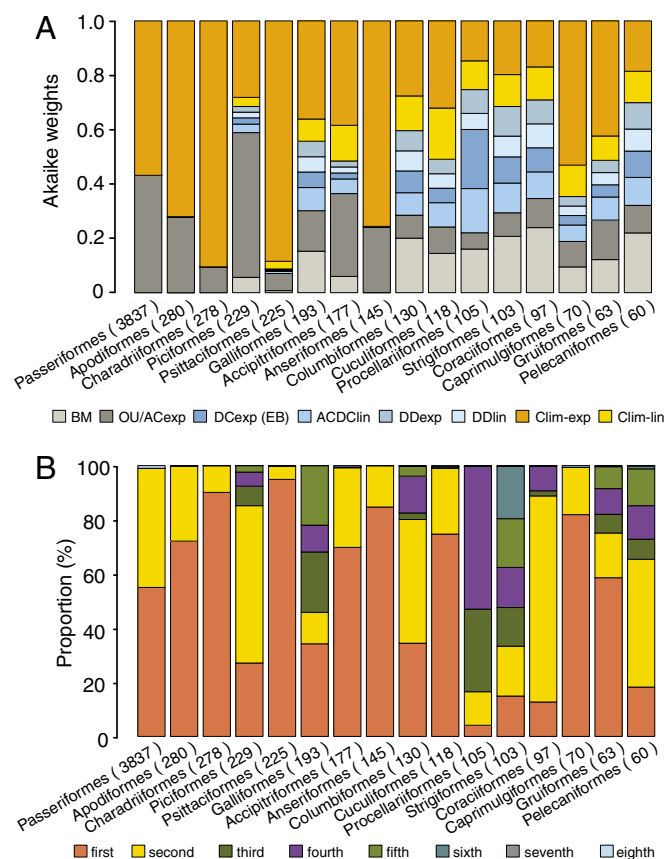


Fig. 1. The climatic model outperforms all others (results for birds) (equivalent results for mammals are shown in *SI Appendix*, Figs. S17 and S18). (A) The height of each colored bar represents the relative support for each model (mean Akaike weight over 1,000 trees from the posterior distribution). (B) The height of each bar represents the proportion of trees from the posterior distribution for which the Clim-exp model is ranked first to last. OU is equivalent to ACexp. ACDClin, linear increase or decrease; DCexp, exponential decrease; DDexp, exponential diversity dependence; DDlin, linear diversity dependence; EB, early burst.

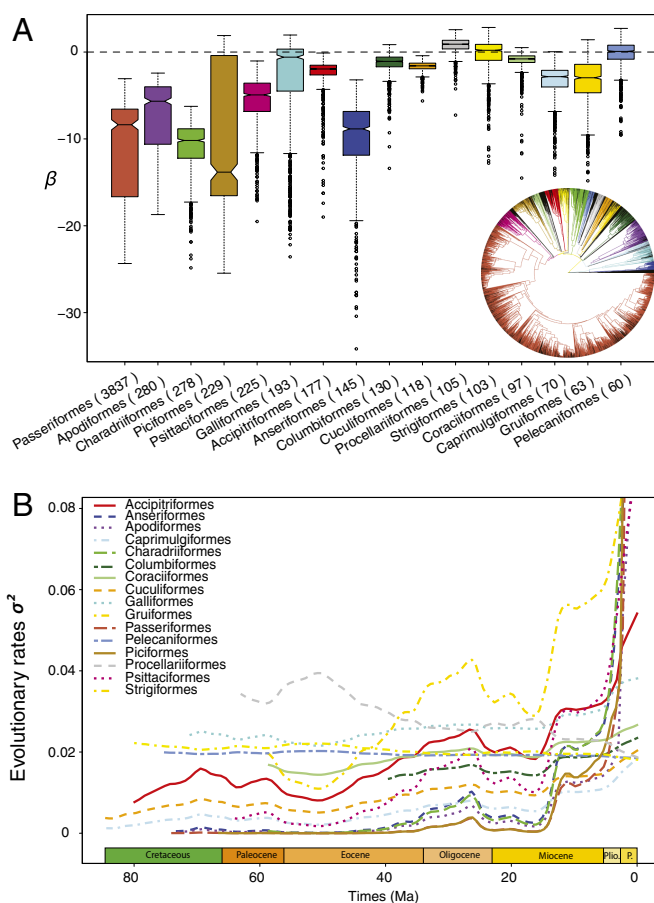


Fig. 2. (A) Rates of body size evolution are negatively associated with temperature in most bird orders (equivalent results for mammals are shown in *SI Appendix*, Figs. S17 and S18). Boxplots represent, for each bird order, the median, the first and third quartiles, and extreme values of estimated β values for 1,000 trees from the posterior distribution; β measures the strength and direction of the temperature dependency of evolutionary rates. The different clades are represented on the complete bird phylogeny (9,993 species); species that were not included in the analyses are represented in black. (B) Rate through time curves for each bird order obtained using median estimates of β over the posterior distribution of trees (equivalent results for mammals are shown in *SI Appendix*, Fig. S19). Body size evolution consistently accelerates during the Oligocene cold period and from the mid-Miocene to the recent past. Plio., Pliocene; P, Pleistocene.

were poorly supported. The inferred negative exponential association between rates of body size evolution and temperature implies that these rates increased during the cold climatic periods of the Cenozoic, such as the Oligocene and late Miocene (Fig. 2B and *SI Appendix*, Fig. S19).

The support for the Clim-exp model with negative β held across posterior distributions of trees, the two distinct phylogenies that we used for mammals, and major bird and mammalian families, suggesting that these results were robust to phylogenetic uncertainty and taxonomic scale (Figs. 1 and 2 and *SI Appendix*, Figs. S16–S18). In addition, we tested whether the well-known tendency for increasing body size over evolutionary time [Cope's or Depéret's rule (22, 23)] could artificially favor the support of our climatic model (*Materials and Methods*) and found that it was not the case (*SI Appendix*, Fig. S20).

Previous studies reporting a tendency for increasing rates of body size evolution through time have attributed this increase to episodic and short-term bursts of evolution (24, 25). Simulating data with randomly distributed episodic bursts (*Materials and Methods*), we found that it is unlikely that rate shifts confined

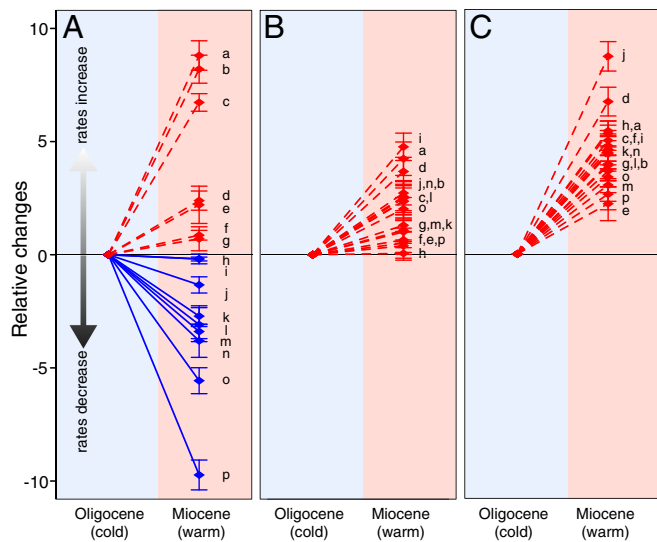


Fig. 4. ME cannot explain rate differences between the cold Oligocene period (33.9–25 Ma) and the following warm period (25–16 Ma) spanning most of the early to mid-Miocene (*SI Appendix, Figs. S27 and S28*). Rate differences ($\log \sigma_{warm} - \log \sigma_{cold}$ mean over 1,000 trees from the posterior distribution; error bars represent the 95% confidence intervals on the mean rate differences) estimated on (A) empirical data, (B) data simulated under the Brownian process with ME, and (C) data simulated under the OU process with ME. MEs bias evolutionary rate estimates toward increasing values from the Oligocene to the following early to mid-Miocene period (red), whereas around one-half of the empirical datasets show decreasing values (blue). Some of the trends found in this analysis differ from those obtained with the climatic model (e.g., for the Procellariiformes and Anseriformes); these apparent contradictions are discussed at length in *SI Appendix*. a, Anseriformes; b, Gruiformes; c, Piciformes; d, Galliformes; e, Pelecaniformes; f, Charadriiformes; g, Strigiformes; h, Passeriformes; i, Columbiformes; j, Apodiformes; k, Accipitriformes; l, Coraciiformes; m, Cuculiformes; n, Caprimulgiformes; o, Psittaciformes; p, Procellariiformes.

exclude the possibility that it is not cold average temperature per se but rather, that it is its correlation with high geographical and/or temporal climatic heterogeneity that spurs phenotypic divergence (37, 38).

It has been proposed that the disparity in body sizes that we observe today across species within clades accumulated early in clades history (2, 27) or that this disparity results from rare and randomly localized bursts of evolution spread throughout the tree and corresponding to the exploration of new adaptive zones (24, 39). Here, we find that the pace of body size evolution responds to an external climatic forcing that operates on entire clades and across groups as diverse as birds and mammals. Directly interpreting these results in the context of the current climatic changes should be done with caution given that contemporary changes are orders of magnitude faster than historical ones. However, our study highlights global temperature as a manifest driver of evolutionary rates, suggesting that human-driven climate changes will have (or already have had) a major effect on evolution.

Materials and Methods

A General Model of Phenotypic Evolution Accounting for Environmental Variations. To test the effect of past measured environmental variables on rates of phenotypic evolution, we extend the BM process (16–19) with time-varying evolutionary rate $\sigma(t)$:

$$dX(t) = \sigma(t)dB(t), \quad [1]$$

where $dB(t)$ is a white noise with mean = 0 and variance of dt . We allow $\sigma(t)$ to be influenced by one or k environmental variables $E_1(t), E_2(t), \dots, E_k(t)$, which themselves vary through time:

$$\dot{\sigma}(t) = \sigma(t, E_1(t), E_2(t), \dots, E_k(t)). \quad [2]$$

The likelihood corresponding to this model is the classical multivariate normal distribution (18, 40), with the variance–covariance matrix given by

$$V_{ij} = \int_0^{S_{ij}} \bar{\sigma}^2(t)dt = \int_0^{S_{ij}} \sigma^2(t, E_1(t), E_2(t), \dots, E_k(t))dt, \quad [3]$$

where S_{ij} represents the time between the root and the most recent common ancestor of species i and j (e.g., ref. 41 has related models). To speed up the computation of the likelihood, we used a stretching–pruning approach, which consists of transforming (stretching) the branches of the tree according to the expected variance–covariance (42) before computing the likelihood recursively using a fast dynamic algorithm based on independent contrasts (pruning) (40, 43, 44). The integrals 3 were computed numerically using the Gauss–Kronrod quadrature formula (45) implemented in the “integrate” function from the stats R base package (46). Finally, maximum likelihood optimization was performed using the quasi-Newton method (47) (L-BFGS-B) implemented in the “optim” function in R. These implementations are available in the RPANDA package (48) publicly available from the CRAN repository (function *fit.t.env*). They can be used on both ultrametric and nonultrametric trees, therefore allowing the possibility to analyze combined fossil and extant data.

We applied this general model to test if and how rates of phenotypic evolution are related to changes in temperature T . We scaled the temperature curve between zero and one; in what follows, T stands for scaled temperature. We considered two simple models relating phenotypic rates σ^2 to temperature T either linearly [$\sigma^2(t) = \sigma_0^2 + \beta T(t)$ (the Clim-lin model)] or exponentially [$\sigma^2(t) = \sigma_0^2 e^{\beta T(t)}$ (the Clim-exp model)], where σ_0^2 is the hypothetical clade-specific phenotypic rate at an average global-scale temperature of 0°C and β reflects the strength and direction of the dependency to temperature. In these models, rates of phenotypic evolution are increasing with increasing temperature when β is positive, are decreasing otherwise, and reduce to a constant rate BM when $\beta = 0$. For computational convenience, the Clim-lin model was parameterized as $\sigma^2(t) = \sigma_0^2 + (\beta - \sigma_0^2)T(t)$, such that with a scaled temperature curve, σ^2 is made up between σ_0^2 and β , increasing with temperature when $\beta > \sigma_0^2$ and decreasing with temperature when $\beta < \sigma_0^2$ (49). We thoroughly tested the ability of our approach to recover input parameters using extensive simulations (*SI Appendix*).

Model Comparison. We compared the fit of the climatic models with six competitive models of trait evolution. We fitted the classical BM and an Ornstein–Uhlenbeck (OU) process, which both assume a constant diffusion σ (50, 51). On ultrametric trees and assuming that the root state is at the optimal trait value, the likelihood of the OU model is identical to a time-dependent model with σ increasing exponentially with time [known as the accelerating rate (AC) model (52); we name it the exponential increase (ACexp) model here for clarity]. We, therefore, refer to this process as the OU/ACexp process. We also consider a time-dependent model with σ decreasing exponentially with time [the early burst model (41, 53); we name it the exponential decrease here for clarity] and a time-dependent model with σ varying linearly with time either positively or negatively (4, 41) (coined linear increase or decrease). Finally, we consider the two models that have been used so far to model diversity-dependent effects, with σ constrained to decay with the number of lineages (3, 4) either exponentially (exponential diversity dependence) or linearly (linear diversity dependence). The relative statistical support for the various models was assessed using the Akaike weights (54). We thoroughly assessed the statistical properties of our model comparison framework using intensive simulations (*SI Appendix*). In particular, we tested our ability to recover the climatic model when it was the generating model and also, that it was not spuriously detected when it was not the generating model.

Body Size Data. We extracted body mass estimates (in grams) for 9,993 bird species from the EltonTraits 1.0 database (55) and 3,574 mammal species from the PanTHERIA 1.0 database (56). We discarded estimates for 261 bird species that were based on genus or family mean values and that could have biased our evolutionary rate estimates. Body mass estimates were log-transformed before analysis.

Phylogenetic Trees. Bird phylogenies were taken from the recently updated (v2.ii) (57) posterior distribution by Jetz et al. (58), from which we discarded species that did not have molecular information. Mammal phylogenies were taken from two sources. The first consisted of 1,000 trees sampled from the pseudoposterior distribution by Kuhn et al. (20), which was obtained by randomly resolving polytomies from the widely used supermatrix tree by Bininda-Emonds et al. (59). Because these random polytomy

resolutions could inflate evolutionary rate estimates and bias our results (60–62), we also conducted all of our analyses on 1,000 trees from the posterior sample ($v.1.002$) of a recently published phylogeny of 4,160 extant mammal species by Faurby and Svenning (21) largely based on sequence alignments and ages by Meredith et al. (63). However, Faurby and Svenning (21) focused on resolving topological conflicts rather than branch length, and the authors themselves caution against interpreting branch lengths in their phylogeny. Thus, although the two phylogenies supported consistent results, we reported results for only the birds in the text.

We aligned the phylogenetic and body size data; to test the robustness of our results to taxonomic scale, we conducted analyses at both the order and family levels. We dismissed phylogenies with less than 50 species, because results from simulations showed that a minimum of 50 species was necessary to be able to statistically distinguish our climatic models from other models (SI Appendix). For birds, this alignment resulted in the analysis of 16 orders and 36 families, representing a total of 6,110 species. For mammals, this alignment resulted in the analysis of 12 orders and 15 families, representing a total of 3,355 species [11 orders and 12 families representing a total of 2,664 species for the trees by Faurby and Svenning (21)].

Temperature Data. We used the temperature curve by Cramer et al. (14). Similar to the more widely used Zachos curve (13), the curve by Cramer et al. (14) is derived from benthic foraminiferal (bf) $\delta^{18}O_{bf}$ isotopic ratio. However, contrary to the Zachos curve, the curve by Cramer et al. (14) accounts for fluctuations in sea water (sw) $\delta^{18}O_{sw}$ through time, which is important for periods of large-scale glaciations when differences in $\delta^{18}O_{sw}$ can go up to -1.11‰ in Vienna Standard Mean Ocean Water (VSMOW) (64). In addition, the curve by Cramer et al. (14) provides temperature estimates for the last 108 My, thus spanning the full time range over which extant bird and mammal orders originated. Although this curve is derived from the marine record, it correlates well with the more fragmented continental record (65). Rather than local or seasonal fluctuations, these curves reflect planetary-scale climatic trends that are expected to have led to temporally coordinated changes in several clades (7, 9, 66).

Simulating Cope's Rule. We simulated Cope's or Depéret's rule (23)—the general tendency for increasing body sizes through time—to check whether this trend could artificially favor the support of our climatic model. We simulated evolution toward larger size as taxa chasing an increasing size optimum (67) using a generalization of the OU model (also called Hull–White model) (4):

$$dX(t) = \alpha [\theta(t) - X(t)] dt + \sigma dB(t). \quad [4]$$

We simulated an adaptive optima changing either linearly through time according to $\theta(t) = \theta_0 + \mu t$ or linearly as a function of temperature $\theta(t) = \theta_0 + \mu T(t)$ according to Bergman's rule (15, 22). Our simulations were run on the phylogenies corresponding to each order with two sets of parameter values. We chose α values corresponding to a phylogenetic half-life [time for the OU process to reach one-half the time to stationarity (50)], representing 10 and 100% of the tree height; σ was chosen to be 2α times the observed trait variance [as expected under the stationary condition (50)], and μ was fixed to 0.02 (-0.02 in the case of the optima tracking temperature). Simulations were performed recursively using a forward algorithm from the root to the tips using our own code.

Assessing the Effect of Episodic Bursts of Phenotypic Evolution. It has been proposed that phenotypic evolution in most vertebrate groups proceeds by rare but substantial bursts along isolated branches (24, 39) [from a 2- to a 52-fold increase, with median value around five in the mammalian supertree (figure 1B in ref. 24)] and that such bursts might drive the support of homogeneous models estimated over entire clades (24). We believe this to be unlikely, because the pattern of interspecific covariances for a process of punctuated evolution with large normally distributed changes is

expected to be almost nondifferentiable from that of a BM process (18). We nevertheless tested the possibility that localized shifts in trait evolution artificially favor support for our climatic models using simulations. For each order-level phylogeny, we performed 1,000 simulations of Brownian evolution with localized shifts in σ . Each simulation consisted of randomly selecting edges in the tree where shifts occur (the number of shifts was a proportion ranging from 1 to 10% of the number of species in each order). The amplitude of each shift was drawn from a truncated log-normal distribution with mean = 1.5, variance = 0.5, and lower and upper bounds = 2 and 52, respectively; these parameters reproduce the range of rate increases previously observed on mammals, with a median value around five (24). The simulations were performed by stretching the randomly selected branches according to the selected rate increases before simulating a homogeneous Brownian process with $\sigma^2 = 1$ using the recursive function "rTraitCont" from the R package ape (68). We then fitted eight competitive models to each simulated dataset and compared their relative fits.

Testing Whether Specificities of the Temperature Curve Matter. To test whether the fit of the climatic model could be explained by the overall cooling trend over the Cenozoic rather than specificities of the temperature curve, we assessed the impact of increasingly smoothing the temperature curve on the support of the Clim-exp model. We used cubic splines with a decreasing effective number of dfs to smooth the curve (69). For each degree of smoothing, we computed the proportion of trees from the posterior distribution of 1,000 trees for which the fit with the smoothed climatic curve remains as good as with the original curve ($|AIC_{smoothed} - AIC_{original}| < 4$) (SI Appendix, Figs. S22–S24). The ΔAIC threshold of four represents a useful approximation for the 95% confidence set on the reference (unsmoothed) model (54).

Assessing the Robustness to ME. We used simulations to test if ME in the body size data could artificially drive the observed climatic signal. We first derived empirical distributions of ME for each bird order using data from ref. 70 (SI Appendix). Next, for each order, we simulated tip data under BM and OU on 1,000 trees from the posterior distribution, and on each of these tip data, we added ME drawn from the empirical distribution (SI Appendix). Finally, we conducted our model fitting procedure on the resulting simulated data.

To refine our understanding of what type of climatic signal ME would spuriously create or in contrast, blur, we conducted time bin analyses. For each order, we sliced trees from the posterior distribution into 2.5-Ma time bins using the "make.era.map" function in phytools (71). We then jointly estimated maximum likelihood rates for each time bin using the "mvBM" function in mvMORPH (44). We performed these analyses on the empirical body size data and data simulated under BM and OU and with ME as described above. Finally, we reported estimated differences in rates (both empirical and simulated) corresponding to a cold period spanning most of the Oligocene (33.9–25 Ma) and a warm period spanning from the late Oligocene to the mid-Miocene (25–16 Ma). Average rates on these periods were obtained by computing the mean rates across the corresponding time bins (the periods were approximated to span 35–25 and 25–15 Ma, respectively, to match the time bins). This approach is useful to visually inspect temporal trends and focus on specific time periods; however, the uncertainty around estimates in each time bin is high and hampers the statistical assessment of general climatic effects in contrast to our proposed framework.

ACKNOWLEDGMENTS. We thank Olivier Billaud, Jonathan P. Drury, Eric Lewitus, Odile Maliet, Marc Manceau, Olivier Missa, Graham Slater, and Marius Somveille for helpful comments on the manuscript. This research was supported by European Research Council Grant ERC 616419-PANDA and Agence Nationale de la Recherche Grant ANR ECOEVOBIO (to H.M.).

- Simpson GG (1953) *The Major Features of Evolution* (Columbia Univ Press, New York).
- Schluter D (2000) *The Ecology of Adaptive Radiation* (Oxford Univ Press, Oxford).
- Mahler DL, Revell LJ, Glor RE, Losos JB (2010) Ecological opportunity and the rate of morphological evolution in the diversification of Greater Antillean anoles. *Evolution* 64:2731–2745.
- Weir JT, Mursleen S (2013) Diversity-dependent cladogenesis and trait evolution in the adaptive radiation of the auks (aves: alcididae). *Evolution* 67:403–416.
- Drury J, Clavel J, Manceau M, Morlon H (2016) Estimating the effect of competition on trait evolution using maximum likelihood inference. *Syst Biol* 65:700–710.
- Vrba ES (1993) Turnover-pulses, the red queen, and related topics. *Am J Sci* 293: 418–452.
- Barnosky AD (2001) Distinguishing the effects of the Red queen and Court Jester on Miocene mammal evolution in the northern Rocky Mountains. *J Vertebr Paleontol* 21:172–185.
- Erwin DH (2009) Climate as a driver of evolutionary change. *Curr Biol* 19:R575–R583.
- Benton MJ (2009) The red queen and the court jester: Species diversity and the role of biotic and abiotic factors through time. *Science* 323:728–732.
- Hunt G, Wicaksono SA, Brown JE, MacLeod KG (2010) Climate-driven body-size trends in the ostracod fauna of the deep Indian ocean. *Palaeontology* 53:1255–1268.
- Hunt G, Hopkins MJ, Lidgard S (2015) Simple versus complex models of trait evolution and stasis as a response to environmental change. *Proc Natl Acad Sci USA* 112:4885–4890.

12. Secord R, et al. (2012) Evolution of the earliest horses driven by climate change in the Paleocene-Eocene Thermal Maximum. *Science* 335:959–962.
13. Zachos J, Pagani M, Sloan L, Thomas E, Billups K (2001) Trends, rhythms, and aberrations in global climate 65 Ma to present. *Science* 292:686–693.
14. Cramer BS, Miller KG, Barrett PJ, Wright JD (2011) Late Cretaceous-Neogene trends in deep ocean temperature and continental ice volume: Reconciling records of benthic foraminiferal geochemistry (d18O and Mg/Ca) with sea level history. *J Geophys Res* 116:1–23.
15. Gardner JL, Peters A, Kearney MR, Joseph L, Heinsohn R (2011) Declining body size: A third universal response to warming? *Trends Ecol Evol* 26:285–291.
16. Martins EP (1994) Estimating the rate of phenotypic evolution from comparative data. *Am Nat* 144:193–209.
17. Felsenstein J (1985) Phylogenies and the comparative method. *Am Nat* 125:1–15.
18. Hansen TF, Martins EP (1996) Translating between microevolutionary process and macroevolutionary patterns: The correlation structure of interspecific data. *Evolution* 50:1404–1417.
19. O'Meara BC, Ané C, Sanderson MJ, Wainwright P (2006) Testing for different rates of continuous trait evolution. *Evolution* 60:922–933.
20. Kuhn TS, Mooers AO, Thomas GH (2011) A simple polytomy resolver for dated phylogenies. *Methods Ecol Evol* 2:427–436.
21. Faurby S, Svenning JC (2015) A species-level phylogeny of all extant and late Quaternary extinct mammals using a novel heuristic-hierarchical Bayesian approach. *Mol Phylogenet Evol* 84:14–26.
22. Smith FA, et al. (2010) The evolution of maximum body size of terrestrial mammals. *Science* 330:1216–1219.
23. Bokma F, et al. (2016) Testing for Depéret's rule (body size increase) in mammals using combined extinct and extant data. *Syst Biol* 65:98–108.
24. Venditti C, Meade A, Pagel M (2011) Multiple routes to mammalian diversity. *Nature* 479:393–396.
25. Hopkins MJ, Smith AB (2015) Dynamic evolutionary change in post-Paleozoic echnoids and the importance of scale when interpreting changes in rates of evolution. *Proc Natl Acad Sci USA* 112:3758–3763.
26. Claramunt S, Cracraft J (2015) A new time tree reveals Earth history's imprint on the evolution of modern birds. *Sci Adv* 1:e1501005.
27. Mitchell JS (2015) Extant-only comparative methods fail to recover the disparity preserved in the bird fossil record. *Evolution* 69:2414–2424.
28. Benson RBJ, et al. (2014) Rates of dinosaur body mass evolution indicate 170 million years of sustained ecological innovation on the avian stem lineage. *PLoS Biol* 12:1–11.
29. Moen D, Morlon H (2014) From dinosaurs to modern bird diversity: Extending the time scale of adaptive radiation. *PLoS Biol* 12:1–4.
30. Gillooly JF, Allen AP, West GB, Brown JH (2005) The rate of DNA evolution: Effects of body size and temperature on the molecular clock. *Proc Natl Acad Sci USA* 102:140–145.
31. Wright S, Keeling J, Gillman L (2006) The road from Santa Rosalia: A faster tempo of evolution in tropical climates. *Proc Natl Acad Sci USA* 103:7718–7722.
32. Mittelbach GG, et al. (2007) Evolution and the latitudinal diversity gradient: Speciation, extinction and biogeography. *Ecol Lett* 10:315–331.
33. Bromham L, Woolfit M, Lee MSY, Rambaut A (2002) Testing the relationship between morphological and molecular rates of change along phylogenies. *Evolution* 56:1921–1930.
34. Davies TJ, Savolainen V (2006) Neutral theory, phylogenies, and the relationship between phenotypic change and evolutionary rates. *Evolution* 60:476–483.
35. Moles AT, Ollerton J (2016) Is the notion that species interactions are stronger and more specialized in the tropics a zombie idea? *Biotropica* 48:141–145.
36. Lawson AM, Weir JT (2014) Latitudinal gradients in climatic-niche evolution accelerate trait evolution at high latitudes. *Ecol Lett* 17:1427–1436.
37. Cooper N, Purvis A (2010) Body size evolution in mammals: Complexity in tempo and mode. *Am Nat* 175:727–738.
38. Botero CA, Dor R, McCain CM, Safran RJ (2014) Environmental harshness is positively correlated with intraspecific divergence in mammals and birds. *Mol Ecol* 23:259–268.
39. Uyeda JC, Hansen TF, Arnold SJ, Pienaar J (2011) The million-year wait for macroevolutionary bursts. *Proc Natl Acad Sci USA* 108:15908–15913.
40. Felsenstein J (1973) Maximum-likelihood estimation of evolutionary trees from continuous characters. *Am J Hum Genet* 25:471–492.
41. Harmon LJ, et al. (2010) Early bursts of body size and shape evolution are rare in comparative data. *Evolution* 64:2385–2396.
42. O'Meara BC (2012) Evolutionary inferences from phylogenies: A review of methods. *Annu Rev Ecol Syst* 43:267–285.
43. Freckleton RP (2012) Fast likelihood calculations for comparative analyses. *Methods Ecol Evol* 3:940–947.
44. Clavel J, Escarguel G, Merceron G (2015) mvMORPH: An R package for fitting multivariate evolutionary models to morphometric data. *Methods Ecol Evol* 6:1311–1319.
45. Piessens R, deDoncker Kapenga E, Uberhuber C, Kahaner D (1983) Quadpack: A Subroutine Package for Automatic Integration, Series in Computational Mathematics V.1 Edition (Springer, Berlin).
46. R Core Team (2016) R: A Language and Environment for Statistical Computing (R Foundation for Statistical Computing, Vienna). Available at <https://www.R-project.org/>.
47. Byrd RH, Lu P, Nocedal J, Zhu C (1995) A limited memory algorithm for bound constrained optimization. *SIAM J Sci Comput* 16:1190–1208.
48. Morlon H, et al. (2016) RPANDA: An R package for macroevolutionary analyses on phylogenetic trees. *Methods Ecol Evol* 7:589–597.
49. Cantalapiedra JL, et al. (2013) Dietary innovations spurred the diversification of ruminants during the Cenozoic. *Proc Biol Sci* 281:20132746.
50. Hansen TF (1997) Stabilizing selection and the comparative analysis of adaptation. *Evolution* 51:1341–1351.
51. Butler MA, King AA (2004) Phylogenetic comparative analysis: A modeling approach for adaptive evolution. *Am Nat* 164:683–695.
52. Uyeda JC, Caetano DS, Pennell MW (2015) Comparative analysis of principal components can be misleading. *Syst Biol* 64:677–689.
53. Blomberg SP, Garland TJ, Ives AR (2003) Testing for phylogenetic signal in comparative data: Behavioral traits are more labile. *Evolution* 57:717–745.
54. Burnham KP, Anderson DR (2002) Model Selection and Multi-Model Inference: A Practical Information-Theoretic Approach (Springer, New York).
55. Wilman H, et al. (2014) EltonTraits 1.0: Species-level foraging attributes of the world's birds and mammals. *Ecology* 95:2027.
56. Jones KE, et al. (2009) PanTHERIA: A species-level database of life history, ecology, and geography of extant and recently extinct mammals. *Ecology* 90:2648.
57. Jetz W, et al. (2014) Global distribution and conservation of evolutionary distinctness in birds. *Curr Biol* 24:910–930.
58. Jetz W, Thomas GH, Joy JB, Hartmann K, Mooers AO (2012) The global diversity of birds in space and time. *Nature* 491:444–448.
59. Bininda-Emonds ORP, et al. (2007) The delayed rise of present-day mammals. *Nature* 446:507–512.
60. Rabosky DL (2015) No substitute for real data: A cautionary note on the use of phylogenies from birth-death polytomy resolvers for downstream comparative analyses. *Evolution* 69:3207–3216.
61. Symonds MR (2002) The effects of topological inaccuracy in evolutionary trees on the phylogenetic comparative method of independent contrasts. *Syst Biol* 51:541–553.
62. Revell LJ, Harmon LJ, Collar DC (2008) Phylogenetic signal, evolutionary process and rate. *Syst Biol* 57:591–601.
63. Meredith RW, et al. (2011) Impacts of the Cretaceous terrestrial revolution and KPg extinction on mammal diversification. *Science* 334:521–524.
64. Lhomme N, Clarke GKC, Ritz C (2005) Global budget of water isotopes inferred from polar ice sheets. *Geophys Res Lett* 32:L20502.
65. Mosbrugger V, Utescher T, Dilcher DL (2005) Cenozoic continental climatic evolution of Central Europe. *Proc Natl Acad Sci USA* 102:14964–14969.
66. Hannisdal B, Peters SE (2011) Phanerozoic earth system evolution and marine biodiversity. *Science* 334:1121–1124.
67. Baker J, Meade A, Pagel M, Venditti C (2015) Adaptive evolution toward larger size in mammals. *Proc Natl Acad Sci USA* 112:5093–5098.
68. Paradis E, Claude J, Strimmer K (2004) APE: Analysis of phylogenetics and evolutions in R language. *Bioinformatics* 20:289–290.
69. Hastie T, Tibshirani R, Friedman JH (2009) The Elements of Statistical Learning, Springer Series in Statistics Edition (Springer, Berlin).
70. Dunning JB (2008) CRC Handbook of Avian Body Masses, ed Dunning JB (CRC, Boca Raton, FL), 2nd Ed.
71. Revell LJ (2012) phytools: An R package for phylogenetic comparative biology (and other things). *Methods Ecol Evol* 3:217–223.